Ecotoxicology and Environmental Safety 259 (2023) 115013

Contents lists available at ScienceDirect

Ecotoxicology and Environmental Safety

journal homepage: www.elsevier.com/locate/ecoenv

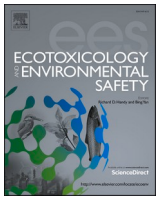

Biodiesel exhaust particle airway toxicity and the role of polycyclic aromatic hydrocarbons

Christopher Ogbunuzor [b], Leonie Francina Hendrina Fransen [a], Midhat Talibi [b], Zuhaib Khan [b], Abigail Dalzell [a], Adam Laycock [a], Daniel Southern [b], Aaron Eveleigh [b], Nicos Ladommatos [b], Paul Hellier [b], Martin Oliver Leonard [a,*]

[a] Toxicology Department, UK Health Security Agency, Harwell Campus, OX11 0RQ, UK
[b] Department of Mechanical Engineering, University College London, Roberts Building, Torrington Place, London WC1E 7JE, UK

ARTICLE INFO

Edited by Dr Yong Liang

Keywords:
Pollutant
Lung
Epithelial
Biodiesel
Particulate matter

ABSTRACT

Renewable alternatives to fossil diesel (FD) including fatty acid methyl ester (FAME) biodiesel have become more prevalent. However, toxicity of exhaust material from their combustion, relative to the fuels they are displacing has not been fully characterised. This study was carried out to examine particle toxicity within the lung epithelium and the role for polycyclic aromatic hydrocarbons (PAHs). Exhaust particles from a 20% (v/v) blend of FAME biodiesel had little impact on primary airway epithelial toxicity compared to FD derived particles but did result in an altered profile of PAHs, including an increase in particle bound carcinogenic B[*a*]P. Higher blends of biodiesel had significantly increased levels of more carcinogenic PAHs, which was associated with a higher level of stress response gene expression including CYP1A1, NQO1 and IL1B. Removal of semi-volatile material from particulates abolished effects on airway cells. Particle size difference and toxic metals were discounted as causative for biological effects. Finally, combustion of a single component fuel (Methyl decanoate) containing the methyl ester molecular structure found in FAME mixtures, also produced more carcinogenic PAHs at the higher fuel blend levels. These results indicate the use of FAME biodiesel at higher blends may be associated with an increased particle associated carcinogenic and toxicity risk.

1. Background

To reduce the reliance on fossil fuels, renewable alternatives have been suggested as part of the strategic move to net zero carbon emissions, and has led many countries to adopt policy initiatives to actively encourage their uptake (Parliament, 2009). Current alternative renewable fuels for diesel engines are mainly comprised of fatty acid methyl esters (FAMEs), commonly referred to as biodiesel (Hellier and Ladommatos, 2015). As these alternatives become more prevalent, it is important to understand how resulting changes in pollutant emissions may impact human health. Indeed, the presence of oxygen within the fuel molecular structure of these fuels, can reduce the production of some regulated pollutants such as CO and total particulate matter (PM), while increasing others such as NO_2 (Hellier et al., 2018; Eveleigh et al., 2016). Despite such observations, much is still unknown regarding the overall relative toxicity of biodiesel versus fossil diesel exhaust pollution.

A limited number of studies focussed to direct human exposure, have attempted to understand the health impacts of biodiesel emissions. Human chamber studies have demonstrated no difference in lung

Abbreviations: FAMEs, Fatty acid methyl ester(s); SME, Soy methyl ester; PM, Particulate matter; PM2.5, PM with a mean aerodynamic diameter of < 2.5 μm; PAHs, Polycyclic aromatic hydrocarbon(s); IARC, International Agency for Research on Cancer; AHR, aryl hydrocarbon receptor; THC, Total Hydrocarbons; OC, Organic carbon; FD, Fossil diesel; NIST, Standard PM reference material SRM2975; NIST.E, Standard PM extract reference material SRM1975; DCM, Dichloromethane; B20, SME Biodiesel blend 20% v/v; B50, SME Biodiesel blend 50% v/v; B100, SME Biodiesel 100% v/v; HDM, House dust mite; B[*a*]P, D[ah]A, B[*b*]F, CRY, NPH; PM.R, Particulate matter without semi-volatiles; ICP-MS, Induced coupled plasma mass spectrometry; MD, Methyl decanoate; M20, Methyl decanoate blend 20% v/v; M50, Methyl decanoate blend 50% v/v; M100, Methyl decanoate 100% v/v; DEP, Diesel exhaust particles; EGR, Exhaust gas recirculation; FAEE, Fatty acid ethyl esters.

* Correspondence to: Toxicology Department, Radiation, Chemical and Environmental Hazards Directorate, UK Health Security Agency, Harwell Campus, OX11 0RQ, UK.

E-mail address: martin.leonard@ukhsa.gov.uk (M.O. Leonard).

https://doi.org/10.1016/j.ecoenv.2023.115013
Received 6 February 2023; Received in revised form 10 May 2023; Accepted 11 May 2023
Available online 13 May 2023

function when compared to fossil diesel exhaust exposure (Mehus et al., 2015; Unosson, 2014). A similar study examining acute cardiovascular outcomes also did not reveal significant effects (Unosson et al., 2021). Epidemiological evidence has thus far been limited to one study in children and suggests lung function decline may occur in those with severe asthma after exposure to biodiesel emissions (Adar et al., 2015). The lack of such studies in humans is a testament to their difficulty, and while informative, their scope is typically limited, focussing mainly on acute physiological health metrics. Much of what we do understand of the likely impacts of changing air pollution emissions with biodiesel comes from direct pollutant measurements and toxicological investigation. *In vivo* toxicology investigations of biodiesel exhaust effects have focussed predominantly on the lung, with some demonstrating increased (Shvedova et al., 2013; Fukagawa et al., 2013) while others decreased or no change (Brito et al., 2010; Douki et al., 2018) in pulmonary effects. *In vitro* analyses have provided the most abundant source of toxicological data and similarly there are no clear conclusions as to the impact on health metrics (Madden, 2016; Southern et al., 2021). Further work in this area is therefore needed, focussed to components of emissions that are altered and that can be mechanistically linked to specific health outcomes. This should not only be limited to regulated pollutants but also include unregulated components with proven bioactivity.

Diesel exhaust is classified by IARC as a class I exposure risk and deemed to be carcinogenic to humans (Silverman, 2018). This classification is based on evaluation of epidemiological studies within the mining and trucking industries among others, where exposures to PM and gaseous material from diesel combustion is high compared to ambient levels. Despite a relatively small proportion of ambient PM2.5 containing diesel exhaust particulates even in areas of high traffic flow (5–6% of total PM2.5 mass; (Kuenen et al., 2021)), the carcinogenic potential of these particulates relative to other toxic air contaminants can be up to 70% of the total risk from ambient air pollution in some cases (Propper et al., 2015). Much if not all of the carcinogenic potential from diesel exhaust particulates has been attributed to particle bound chemicals including polycyclic aromatic hydrocarbons (PAHs) (Claxton, 2015; Ostby et al., 1997; Bostrom et al., 2002).

PAHs are persistent pollutant chemicals produced from incomplete combustion of organic material including fossil fuels, where they act as important precursors in the growth of soot and are found in gaseous form as well as adsorbed onto the exhaust particle surface (Cassee et al., 2013; Li et al., 2016). They have long established toxicological impacts in humans with the lung a major target as the primary site for air pollutant exposure (Lag et al., 2020). Acute effects of PAHs on lung health include asthma and COPD (Smargiassi et al., 2014; Delfino, 2002), while chronic exposure has been directly linked to carcinogenesis of the airway epithelium (Bostrom et al., 2002). The biochemical mechanisms of PAH toxicity involve binding to the aryl hydrocarbon receptor (AHR), which acts as transcription factor to increase expression of phase I and II metabolic enzymes including CYP1A1 and epoxide hydroxylases (Meldrum et al., 2017, 2016). Importantly, this set of metabolic pathway activation can transform PAHs to highly reactive diol-epoxide metabolites, ultimately leading to adduct formation and mutation of DNA underlying their carcinogenicity (Moorthy et al., 2015). This mechanism is considered central to carcinogenicity mechanisms for these chemicals. PAHs have also been observed to result in direct cellular oxidative stress, which can be detected as increased NQO1 and SLC7A11 gene expression in airway cells upon exposure (Meldrum et al., 2016). They have also been observed to modulate mitochondrial function as well as innate and adaptive inflammatory pathways involving IL-1B signalling (Meldrum et al., 2017, 2016; Pardo et al., 2020), which may underlie their effects on inflammatory conditions such as asthma and allergy.

As altered emissions profiles from alternate biodiesel fuels are yet to be fully characterised or understood, there is little systematic knowledge with regards to the overall toxicity of these fuels relative to the fossil fuels that they may displace, particularly with increases in blend ratio. This current study was therefore carried out to address such uncertainties focussed to impacts of diesel combustion derived PM, associated PAHs and their toxicity within the lung. Different blends of soy methyl ester (SME) biodiesel with fossil diesel were combusted at constant engine operating conditions to reduce uncertainties associated with different drive cycle combustion properties across previous studies. The toxicity of these particles was assessed in human primary airway cell cultures. Levels of PAHs adhered to, and elemental composition of PM was measured and investigated as active toxicological constituents. We propose that increased adverse cellular events associated with SME biodiesel PM exposure are attributable to increased levels of the most potent carcinogenic PAHs despite a reduction in total PAH levels. Similar effects on PAH profile were observed for the model fuel FAME, methyl decanoate.

2. Results

As the use of FAME biodiesel continues to rise, it is essential to characterise all possible changes to hazards associated with exhaust material. For many regulated pollutants biodiesel generally reduces the emitted levels, including PM, CO and THC, while increasing NOx. We have previously documented similar changes in these pollutants for SME using the same engine setup and facility used in this study with effects highly dependent on the blend ratio (Hellier et al., 2019; Efthymiopoulos et al., 2019). In addition, there are also reports that biodiesel reduces EC and increases organic carbon (OC) of engine-out PM. Such changes in organic content may indicate changes of toxic chemicals including PAHs. Indeed, reductions in the total PAH content associated with particles of up to 82.9% has been observed in the case of a direct injection diesel generator operated on a SME B20 blend relative to fossil diesel only (Tsai et al., 2011). It was therefore the aim of this study characterise particle bound PAH content from combustion of different blends of SME with reference fossil diesel (FD) and to assess any associated changes in toxicity in airway epithelial cells. Initial characterisation of PM mass per exhaust gas volume from combustion of different SME blends. A lower percentage biodiesel blend formulation B20 (20% (v/v) SME + 80% (v/v) FD), a higher percentage biodiesel blend formulation B50 (50% (v/v) SME + 50% (v/v) FD) and 100% SME biodiesel (B100) were used. Biodiesel use was associated with a decrease in PM levels when compared to FD (Fig. 1A). Next, we analysed particle size properties under conditions used for cell culture treatment (Figure B-C). There was a small SME biofuel dependent increase in particle size metrics (Fig. 1B) when compared to FD and the SRM2975 reference diesel PM (NIST). This may be attributed to the development of secondary larger peaks at ~ 200 nm as can be observed with B100 (Fig. 1C). Evaluation of particle toxicity was carried out using resazurin reduction after treatment of primary bronchial airway epithelial cells for 24hrs (Fig. 1D). NIST particle treatment resulted in a dose dependent decrease in viability (maximal at 150 ug/mL), while there were no significant changes with FD or biodiesel blends. B100 did however reduce viability but not significantly (Fig. 1D). To investigate particle and PAH related toxicity effects in these cells further, we initially established a panel of genes, representative of different stress response pathway activation that have previously been observed as differentially regulated by PAHs including B[*a*]P using RNA-Seq (Meldrum et al., 2016). To validate the capacity of these cells to respond to PAHs, we treated cells with the NIST standard SRM1975 (NIST.E), which is a DCM organic extract of SRM2975 (Fig. 1E). All but one of the chosen genes were differentially regulated. Cells were then exposed to FD, SME blends and NIST standard PM for 24hrs and examined for gene expression changes. 5 genes and their responses, representative of different pathways is displayed (Fig. 1F) with B100 resulting in greater fold changes (upregulated and downregulated) when compared to the effect of FD. The highest regulated gene was CYP1A1, the prototypical AHR dependent gene induced by receptor ligands including PAH molecules. B20 had a less pronounced effect, while NIST displayed a dissimilar pattern

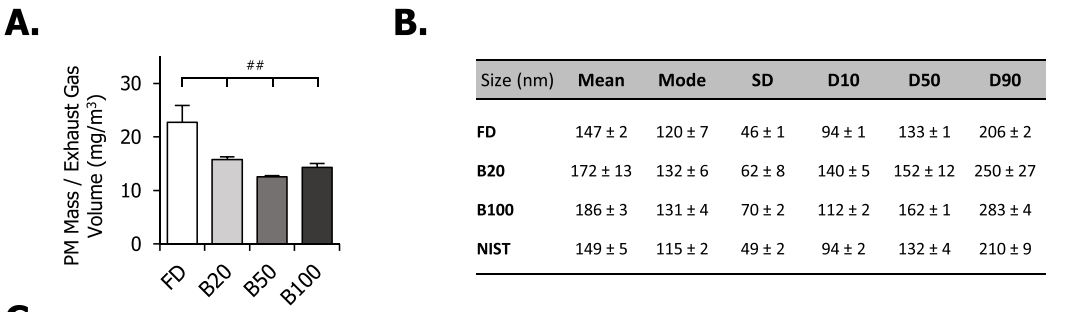

B.

Size (nm)	Mean	Mode	SD	D10	D50	D90
FD	147 ± 2	120 ± 7	46 ± 1	94 ± 1	133 ± 1	206 ± 2
B20	172 ± 13	132 ± 6	62 ± 8	140 ± 5	152 ± 12	250 ± 27
B100	186 ± 3	131 ± 4	70 ± 2	112 ± 2	162 ± 1	283 ± 4
NIST	149 ± 5	115 ± 2	49 ± 2	94 ± 2	132 ± 4	210 ± 9

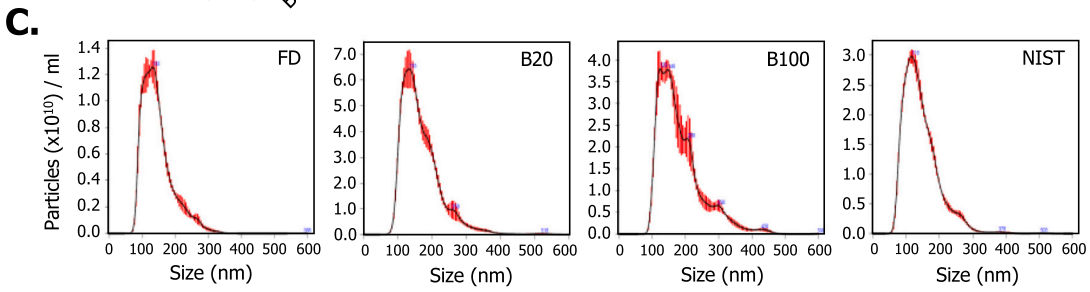

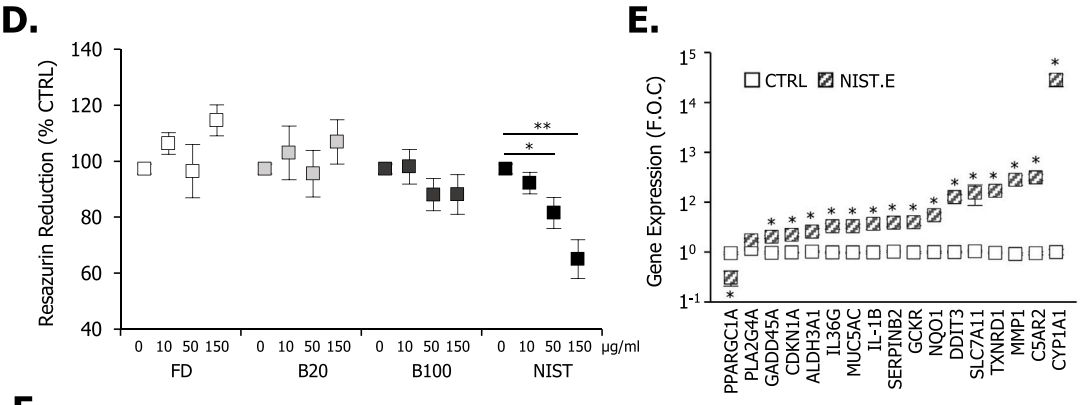

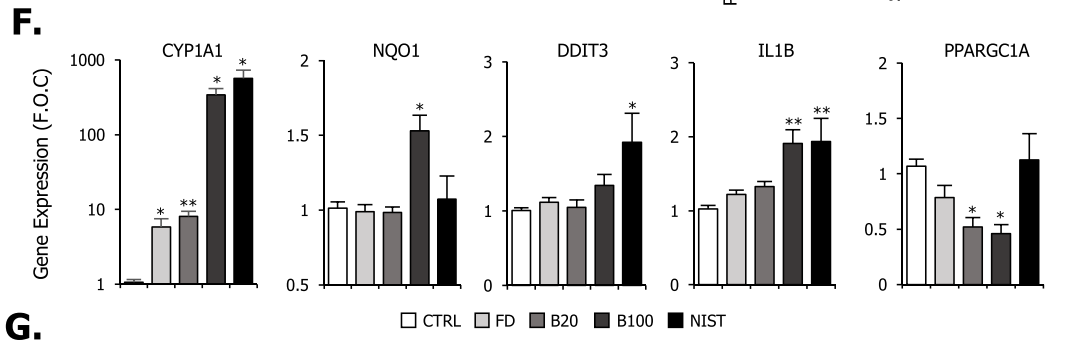

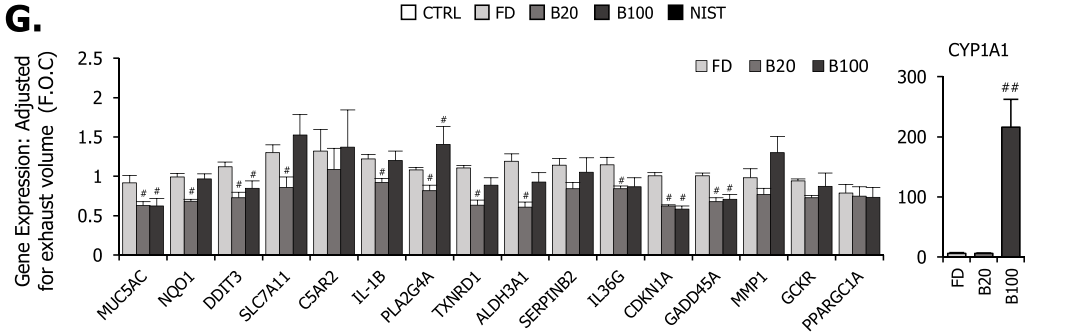

Fig. 1. Impact of biodiesel fuel on exhaust PM characteristics and airway epithelial toxicity. Exhaust PM from a diesel engine run with either Fossil diesel (FD) or neat and blended SME (B20, B50, B100) was collected and assessed for mass per exhaust volume (A) and particle size distribution characteristics when suspended in cell culture media (B-C). These suspensions were also assessed for toxicity in human normal primary airway epithelial cells (n = 6 different donors) using resazurin reduction (D) and PCR analysis of gene expression (F-G) after 24hrs treatment (0–150 µg/mL PM). NIST standard diesel exhaust PM (SRM2975) (NIST) or organic extract material ((SRM1975) (NIST.E) were also examined for toxicity endpoints (D-F). Gene expression is displayed as mean + /- SEM normalised to PM content (D-F) or to exhaust volume (G) as fold over control (F.O.C.). Statistical analysis is one way ANOVA with Fisher LSD post-test (vs *CTRL;* * = <0.05, ** = <0.01. vs *FD;* # = <0.05, ## = <0.01).

of expression to other particle treatments indicative of a fundamentally different particle composition. Additional gene expression changes are displayed in supplementary Fig. 2C and reveal B100 to have the greatest impact when compared to the effect of FD particulates. Confirmation of gene changes was also performed with additional engine test runs (Supplementary Fig. S4). Gene expression fold changes were then normalised to exhaust gas volume rather than PM mass exposures, in order to assess overall relative health risk of exhaust material with the use of different fuel types (Fig. 1G). While the majority of genes displayed non-significant differences in fuel type PM effects, CYP1A1 levels remained elevated in B100 exposed cells. It is acknowledged that these results have focussed on mRNA levels alone rather than analysis of downstream protein expression. We have used this approach to indicate chemical reactivity within the cells and attribute pathway activation, that may be linked to specific chemical classes or properties (e.g. PAH binding to AHR and the induction of gene expression).

Thus far, we have examined in vitro toxicological responses in airway cells from normal human donors with no underlying pathology or disease status. However, the adverse effects of air pollution particulates including those derived from diesel combustion more readily impact those individuals with underlying susceptibilities, including asthma and respiratory allergies (Stevens et al., 2020; Ryu et al., 2020; Meldrum et al., 2020). Therefore, we next compared toxicological responses of different biodiesel exhaust particulates in conditions of house dust mite (HDM) allergen co-exposure (Supplementary Fig. S2) and also in donors with an underlying clinical diagnosis of asthma (Supplementary Fig. S3). HDM is mixture of biologically active substances such as endotoxins, dsDNA and chitins which act on epithelial and other cells within the lung to initiate innate immune responses and cellular dysfunction (Post et al., 2012). These responses can initiate sensitisation processes but occur before any adaptive immune system recognition of allergens within the HDM mixture (Post et al., 2012; Calven et al., 2020). Examination of how pollutants modify these initial innate immune and toxic responses indicate how they may influence later sensitisation and exacerbation events. While HDM exposure appeared to reduce resazurin reduction (non-significant), it did not have any significant impact on fuel particulate treatment effects (Supplementary Fig. S2A). Similarly, HDM co-exposure did not significantly impact biodiesel induced changes in gene expression when compared to particulates alone (Supplementary Fig. S2B-C). Comparisons of exhaust particulate resazurin effects in asthma donors compared to normal donors revealed no significant changes for FD and B100 (Supplementary Fig. S3A). However, the decrease in viability observed with NIST in normal donors was not observed in asthma donor exposures. This effect was also seen with NIST and B100 but not FD when treatments were carried out with HDM co-exposure (Supplementary Fig. S3A). As indicated from Supplementary Fig. 2 no HDM dependent changes in gene expression were observed in normal donors, an effect also observed in asthma donors (Supplementary Fig. S3B). Interestingly however there were differential effects to NIST particles with enhanced expression of PLA2G4A, while diminished DDIT3 and MUC5AC responses, when comparing asthma to normal donor cells (Supplementary Fig. S3B). Ultimately the presence of allergen or asthmatic background did not alter toxicity endpoints from biodiesel particle exposure.

With increased toxicity profiles resulting from SME fuel PM in airway cells, consistent with a pattern of increased PAH bioactivity, it was next decided to examine particle associated PAH levels that may explain such effects. Levels of 16 PAHs previously identified as priority chemicals by the US EPA partly due to their potential carcinogenicity in humans were examined after extraction from PM (Fig. 2). Individual PAH levels per mass of particulate for FD, B20–100 and NIST PM are displayed according to IARC carcinogen classifications with groups 3, 2B, 2 A & 1 representing unclassifiable, possible, probable, and definitive carcinogens in humans respectively. Levels of group 3 PAHs were in the majority of cases significantly reduced with increasing SME blends with the largest reductions observed with B100 vs FD (Fig. 2A). This trend was also observed for some of the group 2B carcinogens (NPH, CRY and B[*a*]A) (Fig. 2B). Interestingly those PAHs with reduced levels upon increasing SME blend were of lower ring number (2−4). In contrast, those group 2B, 2 A and 1 PAHs of 5 ring size (except B[*b*]F) demonstrated clear increases with increasing biodiesel blend when compared to FD. This observation is particularly important given the 2 most potent carcinogens examined (D[ah]A and B[*a*]P) displayed the greatest increase in levels with increased SME blending. These higher levels are still present when results are normalised to exhaust volume (data not shown). A summary of total PAH content (Sum of 16 measured) for each fuel PM is displayed in Fig. 2C and demonstrates decreased levels with increasing biodiesel blend. Analysis of PAH content within the NIST standard particles revealed a general decrease for low molecular weight (low ring number) while an increase in higher molecular weight (large ring numbers) chemicals (Fig. 2A-C). Summary metrics for carcinogenic risk based on equivalency factors of PAH potency relative to B[*a*]P based on review of animal exposure studies (Epa, 2010; Nisbet and LaGoy, 1992), have routinely been used to assess relative risk from environmental PAH mixture exposures. This may be an important exercise, as a reduction in total PAH levels may not equate to a reduction in PAH carcinogen or toxicity risk. Such an analysis was carried out (Fig. 2D-E) using two methods and revealed an initial reduction with B20, increasing with B50 to a maximum with B100 when compared to FD. This was only significant using the TEF method weightings (Fig. 2E). The B100 TEF increase was still present when normalised to exhaust volume.

Having demonstrated that increasing FAME biodiesel displacement of fossil diesel results in increased exhaust particle adverse gene expression effects in airway epithelial cells, which was also paralleled by increased levels of more carcinogenic PAHs, it was next decided to remove the semi-volatile particle bound fraction containing these chemicals and examine the resulting particle toxicity. Particles collected from FD or SME combustion were subjected to a baking protocol to remove the semi-volatile fraction. The size distribution of these particles remained for the most part similar albeit for a moderate increase in some larger particles between 200 and 400 nm (Fig. 3A-B). Particulate matter without semi-volatiles (PM.R) was compared to unprocessed PM for toxicity effects using resazurin and gene expression analysis (Fig. 3C-E). No alterations in resazurin reduction was observed for FD or any biodiesel effects (Fig. 3C). There was however a significant attenuation of biodiesel induced stress responsive genes CYP1A1, NQO1 and IL-1B (Fig. 3D) representing AHR, oxidative/electrophilic stress and inflammatory pathways. This pattern was also observed for many other genes examined (Fig. 3E). The removal of PAHs from particles was confirmed for 7 PAH molecules using GC-MS (Fig. 3F). Toxic metals and other chemicals associated with particles may also account for some or all of the toxicity associated with increased SME biodiesel fuel combustion. ICP-MS was used to further characterise such chemical associations (Fig. 4). Of particular interest was an increase in Cu, Zn, Ni, Pb, Cr, Mn and Sn levels in B20 and B100 particles above those observed with FD, with B100 displaying more than B20 indicating a corelation within the quantity of SME used in the fuel blends. For the most part, levels of these elements were not observed to a similar level within the NIST standard particles and may explain some differences in toxicity between these particles observed in airway cells in this study. It should be highlighted that two elements As and Ce were higher in NIST particles compared B100 and may explain acute resazurin toxicity of NIST not observed with B100 treatments. Furthermore, processing of SME particles to remove semi-volatile organic content in fossil diesel and B20 (FD.R, B20.R) displayed moderate reductions in particle elemental composition. This was not however observed to any great extent when comparing B100 to B100.R indicating that levels of toxic metals are unlikely to account for the airway epithelial toxicity differences observed between processed and unprocessed particles.

We have thus far demonstrated increased biodiesel particle toxicity in airway epithelial cells associated with an increased level of the more potent carcinogenic PAHs. Soy feedstock derived FAME biodiesel

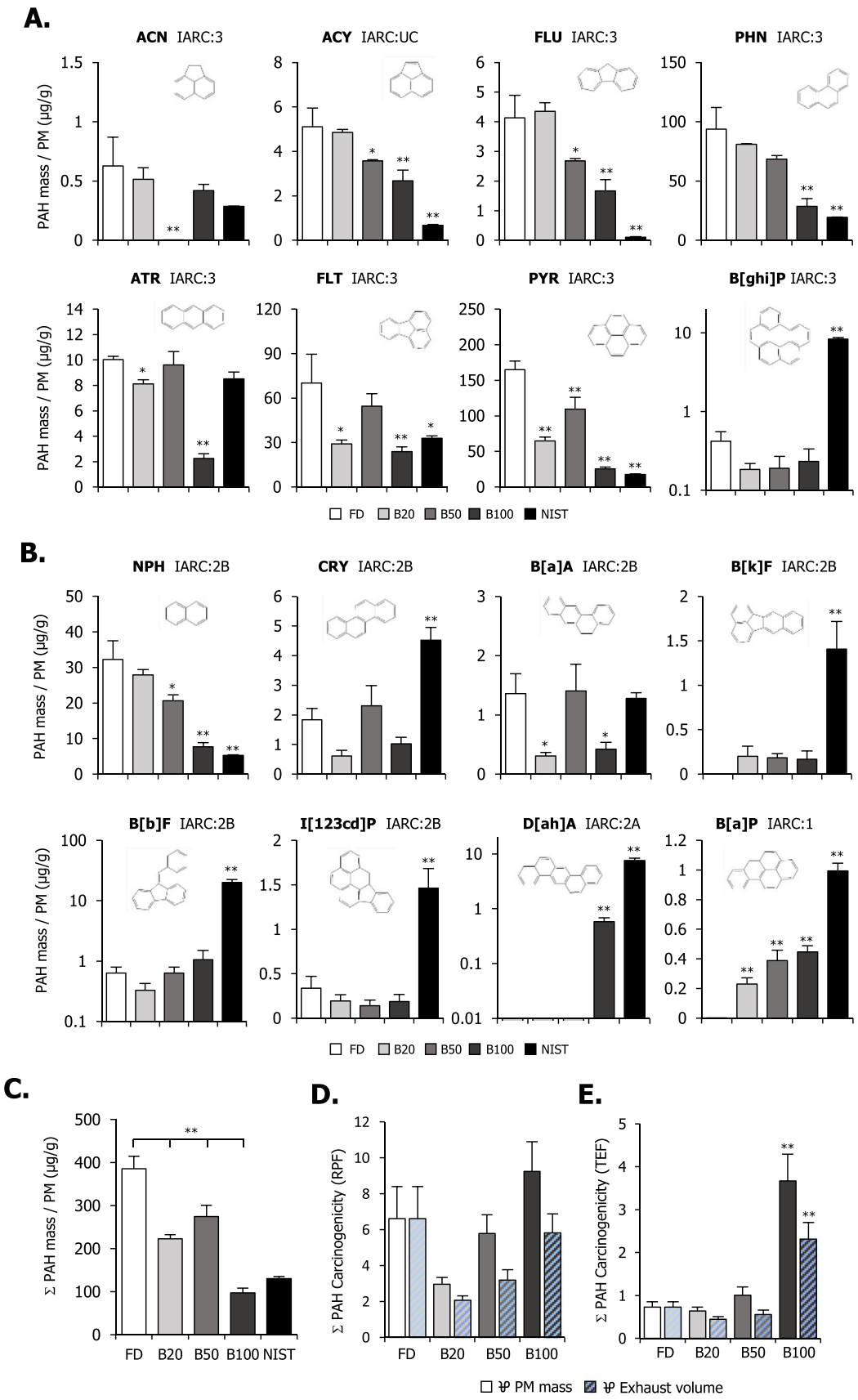

Fig. 2. Impact of biodiesel fuel on exhaust PM PAH content and carcinogenicity relative risk. Exhaust PM from a diesel engine run with either fossil diesel (FD) or neat and blended SME (B20, B50, B100) was collected and analysed for particle bound PAH content using GC-MS (A-B). IARC category 3 carcinogens are displayed (A), while category 2B, 2 A and 1 carcinogens are displayed in panel (B). Total PAH content for the 16 priority PAHs is also displayed (C). Relative carcinogenicity potential was assessed using methods from EPA 2010 (Relative potency factor (RPF)) (D) or Nisbett 1993 (Toxicity equivalent factor (TEF)) (E) with results expressed relative to PM mass or exhaust volume. Results are displayed as mean (n = 3) + /- SEM with statistical analysis was carried out using one way ANOVA with Fisher LSD post-test (vs *FD;* * = <0.05, ** = <0.01).

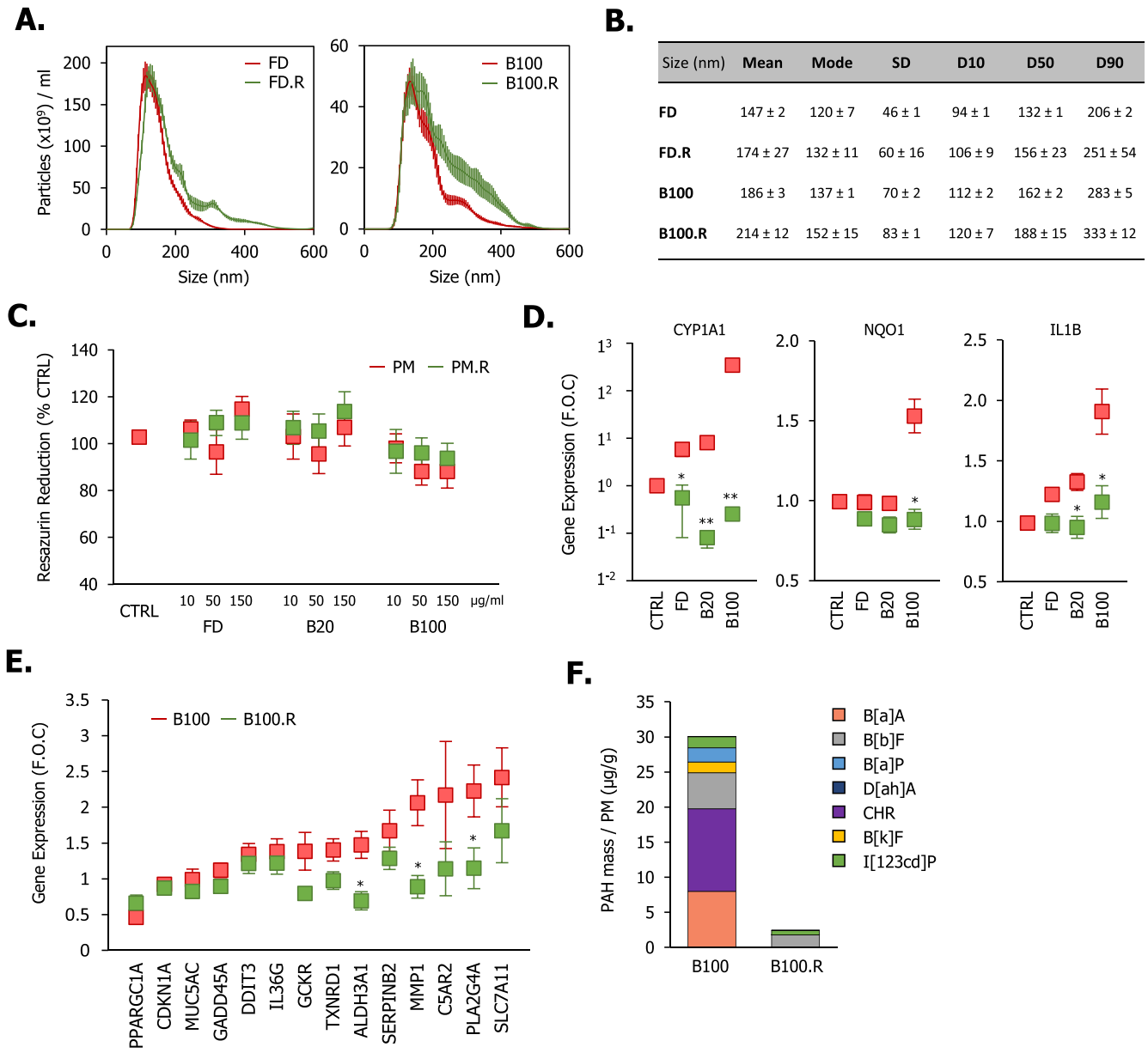

Size (nm)	Mean	Mode	SD	D10	D50	D90
FD	147 ± 2	120 ± 7	46 ± 1	94 ± 1	132 ± 1	206 ± 2
FD.R	174 ± 27	132 ± 11	60 ± 16	106 ± 9	156 ± 23	251 ± 54
B100	186 ± 3	137 ± 1	70 ± 2	112 ± 2	162 ± 2	283 ± 5
B100.R	214 ± 12	152 ± 15	83 ± 1	120 ± 7	188 ± 15	333 ± 12

Fig. 3. Removal of semi-volatile organic content reduces PM airway epithelial toxicity. Exhaust PM from Fossil diesel (FD) and SME (B20, B100) combustion was subject to a baking protocol to remove organic semi-volatile material resulting in particle samples labelled as PM.R, FD.R or B100.R. Particle size distribution characteristics when suspended in cell culture media (A-B) were assessed. These suspensions were also assessed for toxicity in normal human primary airway epithelial cells (n = 6 different donors) using resazurin reduction (C) and PCR analysis of gene expression (D-E) after 24hrs treatment. Gene expression is displayed normalised to PM content as fold over control (F.O.C.) levels. Results are displayed as mean (n = 3) + /- SEM with statistical analysis as students unpaired t-test (vs *un-modified PM for each gene;* * = <0.05, ** = <0.01). PM was also analysed for 7 particle bound PAHs using GC-MS (F).

contains a mixture of different FAME molecules (predominantly C16 to C18 esters) with methyl oleate and methyl linoleate account for > 85% (Fig. 5A). The methyl ester groups on these molecules distinguish them from fossil diesel. Methyl decanoate was chosen for further study as it exemplified the contrasting features of an ester fuel relative to fossil diesel (oxygenated functional group, straight saturated alkyl chain), while possessing physical properties resulting in similar combustion phasing (Supplementary Fig. S4). We next examined whether combustion of a synthetic pure single FAME molecule, methyl decanoate with this same ester group moity (Fig. 5A) would result in similar effects on carcinogenic PAH generation as observed with SME biodiesel. Increasing blends of methyl decanoate with FD (M20, M50, M100) were combusted and the mass of PM per exhaust gas volume was quantified (Fig. 5B). This revealed a decrease in PM mass with increasing methyl decanoate blend. Levels of the most potent carcinogenic PAHs of IARC categories 2B, 2 A and 1 were then measured on these particles using GC-MS (Fig. 5C-D). Similar to effects with SME biodiesel blending, methyl decanoate combustion resulted in PM with increased levels of this PAHs, which was highest for the M50 blend. This was most apparent for B[*k*]F, D[ah]A and B[*a*]P above FD levels. Cumulative quantity of the 16 priority PAHs were also assessed and similar to SME demonstrated decrease in total levels with increasing FAME blend (Fig. 5E), although this was not as pronounced for M20 and M50 as it was for M100. Carcinogenicity relative risk scores were also calculated for methyl decanoate and displayed increased levels for M50 and M100 when calculated per PM Mass (Fig. 5F-G). This increased risk was still present for the M50 blend when factors were normalised to exhaust gas volume (Fig. 5F-G).

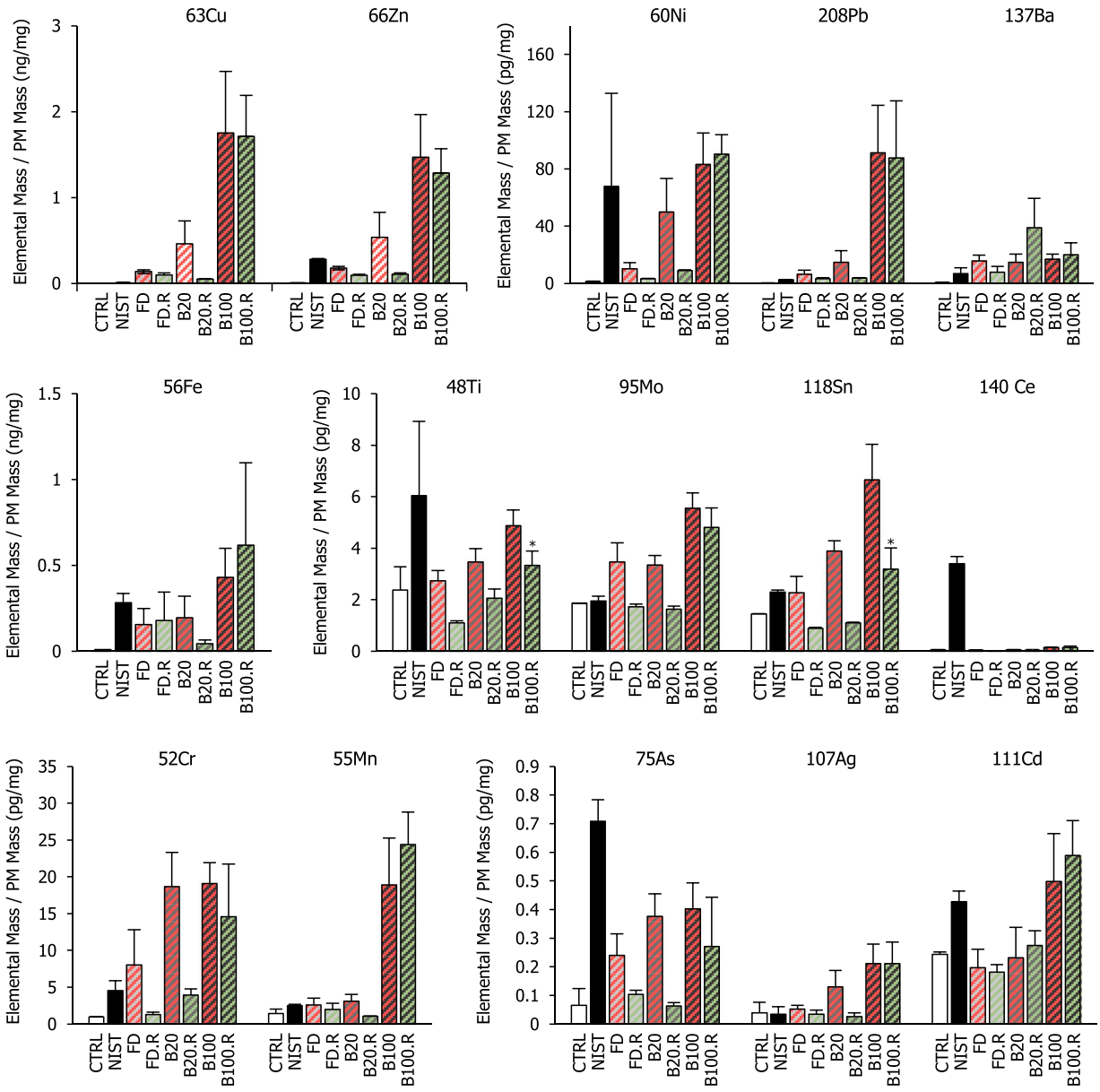

Fig. 4. Elemental composition of PM exhaust material. Exhaust PM from combustion of fossil diesel (FD, FD.R) and SME (B20, B20.R, B100, B100.R) was prepared in cell culture media and subsequently processed for elemental analysis using ICP-MS. Those elements with levels in any PM sample greater than 2-fold over media controls, with 1.5fold difference to FD and with levels above the limit of quantification (LOQ) or limit of detection (LOD) are displayed. Elements with levels below 0.1ppb were also excluded as unlikely to impact toxicity. Results are displayed as mean ng or pg / mg of PM (n = 2 measurements for each particle type, except B100 and B100.R, where n = 5 measurements were taken) + /- SEM. Statistical analysis as students unpaired t-test (B100 vs B100.R; * = <0.05).

3. Discussion

It was the aim of this study to examine the toxicological impact of exhaust emissions arising from increased displacement of FD with FAME biodiesel fuels and to provide some clarity on a generally uncertain assessment of their relative safety, particularly for those emissions components least characterised. As can be seen in our study, the use of biodiesel is associated with a reduction in PM per exhaust gas volume (Hellier et al., 2019; Lapuerta et al., 2008; Shahir et al., 2015), an observation often attributed to the fuel-bound oxygen content and reduced fuel aromaticity of biodiesel blends relative to unblended fossil diesel (Tree and Svensson, 2007; Su et al., 2013). There is however a lack of information on the relative toxicity of these particles, as one cannot assume all combustion particles are alike. Indeed, comparing equal mass of particles from combustion of different fuel types, we observed alterations in stress response genes upon human primary airway epithelial exposure of B100 SME biodiesel particles. This is indicative of adverse cellular impact; an effect not present to the same extent with either FD or a lower percentage blend of SME biodiesel (B20). These increases in transcriptional markers of toxicity are highly unlikely attributable to changes in particle size given the small magnitude of difference between fuel types. In addition, NIST and FD particles have near overlapping profiles of particle size distribution but substantially different responses for viability (resazurin reduction) and gene expression changes. Furthermore, particle processing for organic content removal increased the particle size distribution of the sample, while eliminating gene expression changes, an effect contrary to the suggestion that increased size is responsible for particle bioactivity in this study. Moreover, for genes such as CYP1A1 and ALDH3A1, expression at an mRNA level is driven by chemical ligands of the transcription factor AHR including PAHs and not by particle effects (Bonvallot et al., 2001). Coupled with the fact that DEP extracts (NIST.E) induce a strikingly

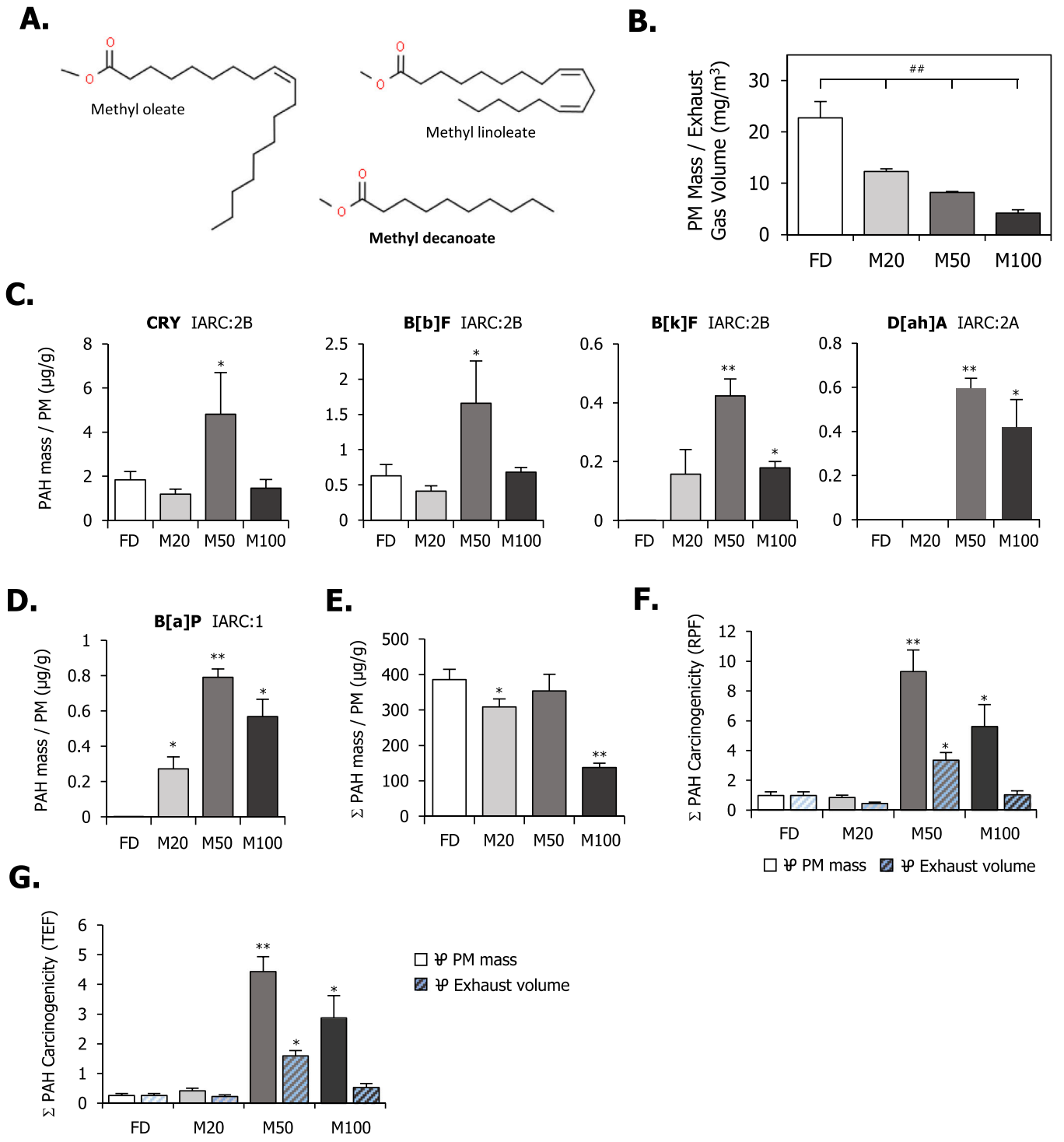

Fig. 5. Impact of methyl decanoate on exhaust PM PAH content and carcinogenicity risk. Molecular structure of primary FAME components of SME (Methyl oleate and linoleate) and model FAME Methyl decanoate are displayed (A). Exhaust PM from a diesel engine run with either fossil diesel (FD) or neat and blended methyl decanoate (M20, M50, M100) was assessed for mass per exhaust volume (B). Particulates were also analysed for particle bound PAH content using GC-MS (C-E). IARC category 2 A and 2B carcinogens are displayed (C), while category 1 carcinogen B[*a*]P is displayed in panel (D). Total PAH content for the 16 priority PAHs is also displayed (E). Relative carcinogenicity potential was assessed using methods from EPA 2010 (Relative potency factor (RPF)) (F) or Nisbett 1993 (Toxicity equivalent factor (TEF)) (G) with results expressed relative to PM mass or exhaust volume. Results are displayed as mean (n = 3) + /- SEM with statistical analysis carried out using one way ANOVA with Fisher LSD post-test (vs *FD;* * = <0.05, ** = <0.01).

similar pattern of gene expression to particle treatments and that removal of semi-volatile material from particles results in significant attenuation or ablation of B100 induced stress response genes, we can be relatively confident that the majority if not all adverse toxicological effects observed in this study can be attributed to particle bound chemicals independent of properties associated with the carbonaceous core.

Even, with this evidence that organic chemicals are responsible for B100 particle effects, other possibilities do exist however, including altered levels of toxic metals. To address this, we used ICP-MS to

investigate particle elemental composition. Using a stepwise screening approach, we identified Cu, Zn, Pb, Sn, Mn and Cd as elements with particle levels above control and FD, which were higher in B100 than B20. Levels of these metals except Sn did not change when particles were processed for organic content removal, a process which removed biological activity, thereby discounting altered levels as causative. With levels of Sn observed in our study within the low pg/mg range, concentrations unlikely to have biological effect (Winship, 1988; Reynolds et al., 2018), we can reasonably discount any role for toxic metals within B100 particles as responsible for the adverse effects observed in our study. It is therefore most likely changes in organic chemical content including PAHs are responsible.

Analysis of particle bound PAH levels was carried out to investigate whether changes in such chemicals account for increased biodiesel particle toxicity. Overall total PAH mass per exhaust PM decreased with increased incorporation of biodiesel fuel. These effects are mainly driven by reductions in more highly abundant smaller ring sized PAHs including naphthalene, phenanthrene and pyrene, which are more often categorised as group 3 (unclassifiable) by IARC, a carcinogenic classification where there is not enough evidence to make a call in humans. In terms of group 2B (possible carcinogens) PAHs, there was a mixed profile of responses with increasing biodiesel use. Importantly however, the two most carcinogenic PAHs in this analysis, D[ah]A categorised as group 2 A (probable carcinogen) and B[*a*]P categorised as group 1 (human carcinogen) were significantly increased with biodiesel use. With changes in multiple PAH molecules of differing carcinogenic potential, attempts have been made to estimate overall carcinogenic risk from complex mixtures based on relative BAP potency metrics calculated from previous carcinogenic studies in rodents (Epa, 2010; Nisbet and LaGoy, 1992). Application of these scores to our data revealed a non-significant decrease at the lower B20 blend and a potential increase in risk for B100, if one uses the TEF method of analysis. Interestingly, this risk was still present for B100 when scores were adjusted for exhaust gas volume indicating a potential for overall increased particle carcinogenic risk when compared to fossil diesel. These results closely parallel those observed for CYP1A1 increases in response to B100, which is important as CYP1A1 is a key initiating event in the mechanism of B[*a*]P carcinogenicity. Further support for PAH profile alterations as a mechanism of increased biodiesel emission particle carcinogenic potential at higher blends comes from combustion experiments using the model single component FAME methyl decanoate. Decreases in total particle PAH levels were paralleled by large increases in levels of D[ah]A and B[*a*]P at M50 and M100 blends. M20 blend modestly increased B[*a*]P similar to B20, again supporting the hypothesis that this type of fuel displacement and biodiesel molecular structure impacts production of these toxins in a similar way. However more work is needed to confirm this. In addition, the PAH carcinogenic index (TEF or RPF) for these analyses of MD demonstrated similar increased carcinogenic risk, which was still significant for M50 when levels were adjusted for exhaust gas volume. Finally, as methyl decanoate has a shorter chain length but retains the same ester moiety, it may be considered the latter to be more important for altered combustion chemical profiles than the former.

While our in vitro toxicology results show some corelation with the levels of more carcinogenic PAH levels, the utility of focussing on just these 16 PAH chemicals as a catch all for this group of toxic chemicals has recently been called into question. This list is a legacy from over 50 years previous and does not contain larger and highly relevant PAHs, alkylated PACs, and compounds containing heteroatoms, which may be present in combustion processes and have toxic effects (Andersson and Achten, 2015). Reliance on these 16 and derived carcinogenic indexes such as TEF may underestimate carcinogenic risk by up to 85% (Samburova et al., 2017).

Beyond PAHs measured in this study there is also evidence that an additional chemical bioactive profile is present within B100 when one compares gene expression results for this exposure against NIST particle effects. Levels of NQO1 were increased with B100, while no change was observed with NIST particle exposure. While levels of the most carcinogenic and bioactive PAHs, BAP and DHA (Meldrum et al., 2016) were higher in NIST than B100 and corelated well with AHR dependent CYP1A1 expression, these levels did not correspond to changes in NQO1. There were in fact no corelation with levels of any of the PAHs measured in this study. Toxic metal effects are also unlikely as causative as NQO1 effects were diminished on semi-volatile fraction removal, where levels of metals remained the same. In addition to NQO1, there was also a significant reduction in a gene responsible for co-ordinating mitochondria biogenesis PPARGC1A (Houten and Auwerx, 2004) with B20 and B100 exposure, again an effect not observed in NIST samples where higher levels of more carcinogenic PAHs (IARC groups 2B, 2A, 1) are present. Removal of particulate organic content reversed in part these reductions in PPARGC1A again indicating a chemical bioactivity beyond classical PAH -AHR activation is present. Interestingly exposure of mice to PM2.5 which contains a fraction of DEPs, has been previously demonstrated to result in airway epithelial mitochondrial vacuolisation, rupture and reduction PPARGC1A expression (Ning et al., 2019). It has also been observed that the polar quinone rich fraction of DEPs, was more potent than the PAH rich aromatic fraction in generating superoxide, mitochondrial pore opening, decreasing mitochondrial mass and induction of apoptosis. These effects which are indicative of mitochondrial toxicity were also observed with ambient air pollutant ultrafine particles but not nanoparticles devoid of chemicals (Xia et al., 2004). Furthermore, as NQO1 is a reductase enzyme specifically tasked with detoxifying quinones (Lee et al., 2021) it is interesting to speculate whether increased expression with B100 exposure may be a specific response to increased levels of this type of toxic chemical on these particles. Indeed, quinones including 1,4-naphthoquinone found on diesel particles have been demonstrated to directly modify mitochondrial function (Xia et al., 2004; Li et al., 2022). Other chemical types including aldehydes may also be responsible for differential effects between particle types examined in this study.

Unlike changes observed with CYP1A1 levels, alterations in NQO1 and PPARGC1A as well as other stress response genes, did not persist when results were normalised to exhaust gas volume, indicating no change in overall inhalation risk for this set of toxicity endpoints when comparing SME to FD. However, this assumption is based only on a single 24 h exposure and is limited to a model of the airway containing only one cell type and the measurement of a limited number of toxicity endpoints. A more in-depth toxicity assessment, coupled with a more comprehensive chemical characterisation of SME particles may yet reveal further risks to airway health through mechanisms beyond those driven by changes in PAHs, CYP1A1 and related AHR activation. Indeed, a recent study in Nature (Hill et al., 2023) has highlighted a novel air pollution particle driven inflammatory mechanism of lung cancer in non-smokers. Increased levels of the main driver of this effect, IL-1B was increased with B100 particle exposure, an effect that could be attributed to the particle bound chemical fraction.

With the alterations in particle bound PAH chemicals observed in this study, it is important to understand how fossil fuel displacement with FAME biodiesels may alter combustion dynamics and what role fuel molecular structure plays. Such properties and associated toxicities will ultimately impact how one may consider incorporating such fuels across society and the inhalation risks that may arise. In analysing the PAHs formed during combustion of a range of FAME and fatty acid ethyl esters (FAEE) at varying oxygen pressures in a bomb calorimeter, Llamas et al (Llamas et al., 2017). proposed production via initial abstraction of a hydrogen from the α-carbon adjacent to the ester group to produce a stable acrylic ester molecule and an alkyl or alkenyl radical, which subsequently decomposes to short chain precursors to aromatic formation, usual soot and PAH precursors. While FAME and FAEE from the same fatty acid feedstock formed similar concentrations and composition of PAH, despite differences in the ester alcohol moiety, lower levels of PAH were produced by more highly unsaturated esters, suggested to be due to the formation of resonance stabilised allenes. It is tentatively

suggested therefore that the effects of SME blend level on the abundance of several PAH apparent in Fig. 2 can be attributed to displacement of the wide range of aromatic ring and soot precursors derived from the various paraffinic, cyclic and aromatic compounds that comprise fossil diesel with a more limited selection of species formed from the biodiesel alkyl moieties. Such a changing composition of PAH precursors may explain the gradual increases and decreases seen in the concentration of some species with increasing SME blend level, for example NAP and B[*a*]P respectively. As to what specific properties of FAME and the combustion route it takes to form more toxic PAHs such as B[*a*]P and D[ah]A as found in this study remains to be elucidated.

It is important to discuss properties of fuel combustion independent of fuel molecular structure that may account for changes in PAH profiles. Supplementary Fig. S1B-C shows the apparent net heat release of pure fossil diesel, unblended SME biodiesel, unblended methyl decanoate and the respective blends of both with fossil diesel (B20, B50, M20 and M50). A reduction in peak heat release rates and a greater proportion of mixing rate-controlled combustion with an increasing level of SME biodiesel is observed (Supplementary Fig. S1B). This agrees with previous studies and can be attributed to the impediment of fuel air mixing with the higher viscosity of the biodiesel relative to fossil diesel (Hellier et al., 2019; Schonborn et al., 2009; Peirce et al., 2013). The decrease in peak heat release, and likely also maximum in-cylinder temperatures reached, could be anticipated to decrease rates of particulate oxidation, while a greater extent of mixing rate controlled combustion, also apparent with the displacement of fossil diesel with methyl decanoate (Supplementary Fig. S1C), might be expected to increase the formation PAH and particulate through pyrolysis reactions (Tree and Svensson, 2007). However, the observed decrease in PM emissions with the displacement with either FAME, are suggestive of a greater influence of the ester molecular structure on pyrolysis reaction rates than that of the fuel physical properties on combustion phasing.

Previous studies of B[*a*]P and D[ah]A in the context of increasing SME content in blends with fossil diesel have focused on collecting particulate samples during standardised drive-cycles. For example, during both urban and extra urban drive-cycles levels of B[*a*]P extracted from particulate matter have been found to decrease with increasing SME content (Karavalakis et al., 2010; Bakeas et al., 2011). However, significant increases in B[*a*]P with increasing SME, in agreement with our own study have also been observed (Karavalakis et al., 2017; Bakeas and Karavalakis, 2013) with various driving conditions. Such drive-cycles necessarily require a variety of both steady state and transient engine operation, resulting in a range of global mixture stoichiometries and temperatures within the combustion chamber during particulate collection, factors which can be expected to influence PAH formation independent of fuel composition (Dandajeh et al., 2017, 2018; Khan et al., 2022; Wu et al., 2006). While we acknowledge that using drive cycles are more representative of real-world emissions generations, they come with the disadvantage of uncertainty around howe different fuels may behave under different combustion phases and difficulty in comparison across studies. By using a standardised steady state approach for which most engine activity occurs, we hoped to provide some further clarity on how Biodiesel fuel molecular structure may alter combustion particle toxicity.

4. Conclusion

We demonstrate that under steady state engine conditions that displacement of FD with SME FAME biodiesel increases exhaust emissions particle toxicity in human primary airway epithelial cells, attributable to changes in more toxic PAH species including B[*a*]P and D[ah]A. Physical particle effects and changes in toxic metals were excluded as causative. Increased levels of these priority carcinogens were also increased when FD was displaced with the single component FAME fuel methyl decanoate. Overall carcinogenic risk, calculated from cumulative PAH quantification, increased at the higher blend levels of FAME fuels, an effect that was still present when levels were adjusted for reductions in total exhaust PM mass with FAME use. This adjustment method, used to provide a level of comparison of exhaust particle inhalation toxicity risk across different fuel use, reduced gene expression increases associated with B100 particle exposure, except for CYP1A1. Induction of this gene is typically driven by PAHs including carcinogenic B[*a*]P and is part of the mechanism of carcinogenicity of this chemical. Such results indicate that at higher blends of FAME biodiesel combustion, exhaust particle associated PAHs may pose a risk of enhanced carcinogenicity and/or toxicity.

5. Methods

5.1. Test fuels

The engine was fuelled by three pure fuels namely reference fossil diesel (FD) without FAME, Soybean oil methyl ester (SME) (100% SME labelled as B100), both purchased from a fuel supplier (Haltermann Carless) and methyl decanoate (MD) obtained from a chemical supplier (Sigma Aldrich). In addition to the pure fuels, SME blends (B20, B50) and MD blends (M20, M50) were prepared with FD at ratios of 20 v/v% and 50 v/v% ester content. Supplementary Table S1 reports the chemical composition and physical properties of the pure fuels, with speciation of the fossil diesel PAH content provided in an earlier work (Ogbunuzor et al., 2021).

5.2. Engine specifications and test procedure

All combustion experiments were undertaken with a naturally aspirated single-cylinder direct injection compression-ignition research engine. Engine components, including head, piston and fuel injector, were taken from a commercially available light-duty diesel engine and in-cylinder geometry preserved, further details of the engine specification are shown in Supplementary Table S2. No exhaust aftertreatment devices or Exhaust Gas Recirculation (EGR) were utilised in these experiments. A schematic diagram of the research engine and exhaust sampling apparatus is presented in Supplementary Fig. S1.

For all engine experiments, the ambient air temperature was maintained at 25 °C, and the engine coolant and lubricating oil were preheated to 70 and 80 °C respectively. After reaching the desired temperatures, the engine was fired with fossil diesel for 10 min to heat the engine to a consistent operating temperature. Filters for the collection of particulates from exhaust gases during engine combustion were prepared by sandwiching a 70 mm glass microfibre filter (0.7 μm Pore size, Fisher Scientific UK) between two 70 mm stainless steel woven wire 500 mesh discs (The Mesh Company UK). Sandwiched filters were desiccated for 12 h and pre-weighed before loading into the filter holder within a bespoke housing located upstream of the vacuum pump and gas meter sampling from the main engine exhaust flow. The filter holder housing and connecting stainless-steel pipes to the exhaust were heated to 250 °C by insulated PID-controlled electric tape heaters to prevent condensation of water vapour and gaseous hydrocarbons.

Particulate samples were collected from the engine exhaust for 15 min under steady state conditions at a constant engine speed of 1200 rpm, with the start of injection (SOI) adjusted throughout to maintain a consistent start of combustion (SOC) at top dead centre where the duration of ignition delay varied with fuel composition. Injection durations were varied between tests to maintain a constant engine load of 7 bar indicated mean effective pressure (IMEP), with all fuels injected at a pressure of 450 bar; fossil diesel was supplied to the injector directly from a common rail, while FAME blends were pressurised and supplied from a novel low volume fuel system (Talibi et al., 2018). Once collected, all sandwiched filters were placed in petri dishes and stored below – 20 °C in the dark in accordance with the US EPA Method TO-13A. Sandwiched filters were further processed as is or baked at 300 °C for 4 h to remove the semi-volatile organic fraction

(Eveleigh et al., 2015), using similar temperature conditions previously utilised with thermodenuders for the same purpose (Jayaratne et al., 2008). Unbaked or baked particle samples were subsequently removed from the mesh for in vitro testing, particle size analysis, elemental composition or processed directly from the filters for PAH analysis.

5.3. Particle extraction and PAH analysis

Particle PAH extraction and analysis was carried out as previously described (Ogbunuzor et al., 2021). In brief, samples were desiccated for 12 h and reweighed to determine the particulate mass recovered. Particle extracts were prepared from the sandwiched filters with dichloromethane (DCM) in a Dionex Accelerated Solvent Extractor (ASE150) under conditions optimised by Dandajeh et al (Dandajeh et al., 2017, 2018).: 125 °C and 103.5 bar for three 5-minute static cycles followed by 4 mL rinse and 60 second nitrogen purge. The combined extract (60–90 mL) from three extractions of each particulate sample was reduced to 1–2 mL in two stages under nitrogen flow. Initially the extract was reduced to 11 mL in the collection bottle and transferred without losses into a preconditioned 15 mL graduated centrifuge tube for further reduction. After reducing to 1–2 mL, the extract was transferred into 2 mL screw cap vials for GC-MS analysis. An Agilent 5977 A GS-MS detector fitted with a Restek fused silica Rxi-17Sil MS column was used to identify and quantify the PAH profile present in the organic extracts. The configuration and operating parameters of the GC-MS are reported in Supplementary Table S3. To quantify the PAH profile, 50 μl of the external standard (2000 μg/mL 16 EPA priority PAH mixture in DCM) was serially diluted with DCM to 1100 μl at four calibration levels: 50, 25, 10 and 5 ppm. To compensate for potential unequal loading of the GC column by the Automatic Liquid Sampler (ALS), 10 μl of internal standard comprised of deuterated PAHs recommended by EPA: Naphthalene-d8, Acenaphthalene-d10, Phenanthrene-d10, Chrysene-d12 and Perylene-d12 was added to each sample and calibration vial. A carcinogenicity metric for particle-phase PAHs was calculated from the 16 measured PAHs and reported as either a Toxicity Equivalent Factor (TEF) or Relative potency factor (RPF) using relative PAH weightings normalised to B[*a*]P as described by Nisbet and LaGoy (Nisbet and LaGoy, 1992) and US EPA 2010 (Epa, 2010) respectively, using Eq. 1.

$$B[a]P_{equivalence} = \sum_{i=1}^{16}((TEF \quad or \quad RPF \quad relative \quad ratios) \times (PAH/PM(\mu g/g))) \tag{1}$$

5.4. Particle elemental composition

Particle sample suspensions at a concentration of 1.5 mg/mL were prepared in LHC-9/DMEM cell culture media containing 0.1% Tween 80. Cell culture media without particles were processed alongside particle samples as blank controls. Samples were digested using a microwave assisted acid digestion approach. 0.666 mL of sample suspension (1 mg of particles) were transferred to microwave digestion vials along with 0.46 mL 65% HNO_3, 0.125 mL 35% HCl, 0.25 mL H_2O_2 and 1.5 mL ultrapure water (UPW). This resulted in a volume of 3 mL and acid matrix of 10% HNO_3 and 1.5% HCl. The samples underwent microwave digestion in an Anton Paar MultiWave Go microwave digestion system, where temperatures were ramped to 180 °C over 10 min and held for a further 20 min. Upon completion samples were transferred to 15 mL trace metal centrifuge tubes and centrifuged at 10,000 rpm for 10 min. The supernatant was diluted 5x using UPW to result in an acid matrix of 2% HNO_3 and 0.3% HCl. Sample solutions were analysed using a Thermo iCAPQ inductively coupled plasma mass spectrometry (ICP-MS) instrument. A mixed element standard was prepared and included Li, Be, B, Na, Mg, Al, si, P, K, Ca, Sc, Ti, V, Cr, Mn, Fe, Co, Ni, Cu, Zn, Ga, Ge, As, Se, Rb, Sr, Y, Zr, Nb, Mo, Ag, Cd, In, Sn, Sb, Cs, Ba, La, Ce, Nd, Sm, Eu, Gd, Tb, Dy, Ho, Er, Tm, Yb, Lu, Hf, Ta, W, Re, Pt, Au, Hg, Tl, Pb, Bi, Th, U. Standard solutions were prepared at the following concentrations of 0.01, 0.05, 0.1, 0.5, 1, 5, 10, 25, 50 and 100 μg/L. Online standard addition of Rh in 2%HNO3 was used as an internal standard. Elemental levels were normalised to NanoSight assessed particle volume within the original samples and expressed as ng or pg / mg of particulate mass.

5.5. Particle Characterisation

Size distribution of particulate samples made up in LHC-9/DMEM cell culture media containing 0.1% Tween 80 was determined using nanoparticle tracking analysis (NanoSight LM10 instrument, NanoSight, Amesbury, UK). Particle were reconstituted in media separately 3 times for each fuel type sample and measured separately to ensure accurate estimation of size distribution. Each sample was measured for a minimum of 60 s and processed using the NTA 3.2 Analytical software. Results are displayed as mean particle diameter size, with standard deviation (SD) as well diameter cut-offs below which contain 10% (D10), 50% (D50) and 90% (D90) of the particle volume within the sample resides.

5.6. Cell culture and treatment protocols

Human primary bronchial epithelial cells (HPBECs) were obtained from 6 normal and 4 asthma donors (Epithelix Sàrl, Suisse) with characteristics as described in Supplementary Table S4 and were maintained at 37 °C in a 5% CO_2 humidified atmosphere. Cells were sub-cultured into 24 well plates using Epithelix cell growth media (Cat# EP09AM) with experimental exposures carried out between passage 2–4. Prior to treatment, cells were differentiated using a 50:50 ratio of LHC-9 and DMEM (High Glucose) culture media (Carlsbad, CA, USA) supplemented with bovine serum albumin 0.5 mg/mL, Bovine pituitary extract, 10 μg/mL, Insulin 1 μg/mL, Transferrin 0.125 μM, Hydrocortisone 0.1 μM, Triiodothyronine 0.01 μM, Epinephrine 2.7 μM, Epidermal growth factor 0.5 ng/mL, Retinoic acid 5 × 10–8 M, Phosphorylethanolamine 0.5 μM, Ethanolamine 0.5 μM, Zinc sulphate 3.0 μM, Penicillin G sulphate 100 U/mL, Streptomycin sulphate 100 μg/mL and $CaCl_2$ 1.0 mM. Other stock components and trace elements were added as indicated (Fulcher and Randell, 2013). Culture in differentiation media was initiated after cells reached confluence (at Day 7 of culture) and carried out for a minimum of 14 days, prior to cell treatment. Media replacement was carried out every 2–3 days. For treatment, particles collected from the engine runs were prepared at a concentration of 1.5 mg/mL in LHC-9/DMEM containing 0.1% Tween-80. Suspensions were sonicated to ensure homogeneity as previously described (Meldrum et al., 2020). NIST Standard diesel particulate matter SRM-2975 was used as a positive control for diesel particle associated PAH cellular effects, elemental and PAH analysis. These particles were collected from an industrial diesel engine powered forklift truck and obtained from a chemical supplier (Sigma Aldrich UK). SRM1975 dichloromethane (DCM) extract of SRM2975 NIST standard particles (NIST.E) was processed to replace DCM with an equal volume of DMSO through evaporation under nitrogen. Cells were treated in 500 μl volume per well, to a range of particle final concentrations (0–150 μg/mL) for 24hrs prior to toxicological assessment using resazurin reduction and PCR analysis of gene expression. Control wells contained 50 μl particle diluent (LHC-9/DMEM containing 0.1% Tween-80). NIST.E was used at a final concentration of 10 μg/mL with 1:1000 dilution of DMSO as solvent control.

5.7. Cellular viability

Resazurin reduction is used as an indicator of cellular reductase activity indirectly as a viability indicator and is based on the conversion to a fluorescent product resorufin (Liu, 1981). After treatment, cells were washed once in 200 μl of 44 μM resazurin (Cat# R7017, Sigma-Aldrich, Gillingham, UK) in cell culture media and incubated with a further

200 μl of resazurin solution for a minimum of 1 h at 37 C. Fluorescence was detected at 540 nm excitation and 590 nm emission.

5.8. RNA isolation and PCR

For gene expression analysis, total RNA was isolated using a silica gel-based RNeasy spin column method (Qiagen, Valencia, CA) and as previously described (Fransen and Leonard, 2021). RNA purity was determined using the nanodrop platform (Thermo Scientific) and cDNA synthesised using a random hexamer dependent protocol and reverse transcriptase as per manufacturer's instructions (Cat# BIO-27036, Bioline Reagents Ltd, UK). cDNA was analysed for gene expression using the QuantStudio™ 6 Flex Real-Time PCR System. PCR Primer sequences for real time PCR are listed in supplementary Table S5. cDNA was amplified for 10 min at 95 °C followed by 40 cycles of 30 s at 95 °C and 30 s at 60 °C. Cycle thresholds (Ct values) were quantitatively assessed using the delta-delta Ct method and normalized to GAPDH control.

5.9. Data handling and statistical analysis

Statistical significance between treatments was carried out using Graphpad Prism with one-way ANOVA and Fisher's LSD Test subsequent to outlier removal using the ROUT method. Results are expressed as mean ± standard error of the mean (SEM) unless otherwise stated.

Ethics approval and consent to participate

Not applicable.

Consent for publication

Not applicable.

Funding

This study is part funded by the National Institute for Health Research (NIHR) Health Protection Research Unit in Environmental Exposures and Health, a partnership between UK Health Security Agency and Imperial College London. The views expressed are those of the author(s) and not necessarily those of the NIHR, UKHSA or the Department of Health and Social Care.

CRediT authorship contribution statement

MOL, AE, MT & PH conceived and designed the experiments. CO, MT, DS, AE and PH carried out engine tests of fuels and collection of particulate matter. MOL & LFHF carried out in vitro toxicity assessment. AL carried out elemental composition of particulates by ICP-MS, while AD conducted NanoSight particle size measurements. CO, ZK and DS carried out particle processing and PAH analysis by GC-MS. MOL, PH and NL wrote and drafted the manuscript. All authors contributed to data analysis and drafting of text and figures. All authors read and approved the manuscript.

Declaration of Competing Interest

The authors declare that they have no known competing financial interests or personal relationships that could have appeared to influence the work reported in this paper.

Data Availability

Data will be made available on request.

Acknowledgements

Not applicable.

Appendix A. Supporting information

Supplementary data associated with this article can be found in the online version at doi:10.1016/j.ecoenv.2023.115013.

References

Adar, S.D., D'Souza, J., Sheppard, L., Kaufman, J.D., Hallstrand, T.S., Davey, M.E., et al., 2015. Adopting clean fuels and technologies on school buses. Pollution and health impacts in children. Am. J. Respir. Crit. Care Med. 191 (12), 1413–1421. https://doi.org/10.1164/rccm.201410-1924OC. ⟨https://www.ncbi.nlm.nih.gov/pubmed/25867003⟩.

Andersson, J.T., Achten, C., 2015. Time to say goodbye to the 16 EPA PAHs? Toward an up-to-date use of PACs for environmental purposes. Polycycl. Aroma Compd. 35 (2–4), 330–354. https://doi.org/10.1080/10406638.2014.991042. ⟨https://www.ncbi.nlm.nih.gov/pubmed/26823645⟩.

Bakeas, E., Karavalakis, G., Fontaras, G., Stournas, S., 2011. An experimental study on the impact of biodiesel origin on the regulated and PAH emissions from a Euro 4 light-duty vehicle. Fuel 90 (11), 3200–3208. https://doi.org/10.1016/j.fuel.2011.05.018. <Go to ISI>://WOS:000295734200008.

Bakeas, E.B., Karavalakis, G., 2013. Regulated, carbonyl and polycyclic aromatic hydrocarbon emissions from a light-duty vehicle fueled with diesel and biodiesel blends. Environ. Sci. -Proc. Imp. 15 (2), 412–422. https://doi.org/10.1039/c2em30575e. <Go to ISI>://WOS:000315397700011.

Bonvallot, V., Baeza-Squiban, A., Baulig, A., Brulant, S., Boland, S., Muzeau, F., et al., 2001. Organic compounds from diesel exhaust particles elicit a proinflammatory response in human airway epithelial cells and induce cytochrome p450 1A1 expression. Am. J. Respir. Cell. Mol. Biol. 25 (4), 515–521. https://doi.org/10.1165/ajrcmb.25.4.4515. ⟨https://www.ncbi.nlm.nih.gov/pubmed/11694458⟩.

Bostrom, C.E., Gerde, P., Hanberg, A., Jernstrom, B., Johansson, C., Kyrklund, T., et al., 2002. Cancer risk assessment, indicators, and guidelines for polycyclic aromatic hydrocarbons in the ambient air (doi:). Environ. Health Perspect. 110, 451–488. https://doi.org/10.1289/ehp.02110s3451.

Brito, J.M., Belotti, L., Toledo, A.C., Antonangelo, L., Silva, F.S., Alvim, D.S., et al., 2010. Acute cardiovascular and inflammatory toxicity induced by inhalation of diesel and biodiesel exhaust particles. Toxicol. Sci. 116 (1), 67–78. https://doi.org/10.1093/toxsci/kfq107. ⟨https://www.ncbi.nlm.nih.gov/pubmed/20385657⟩.

Calven, J., Ax, E., Radinger, M., 2020. The airway epithelium-a central player in asthma pathogenesis. Int. J. Mol. Sci. 21, 23. https://doi.org/10.3390/ijms21238907. ⟨https://www.ncbi.nlm.nih.gov/pubmed/33255348⟩.

Cassee, F.R., Heroux, M.E., Gerlofs-Nijland, M.E., Kelly, F.J., 2013. Particulate matter beyond mass: recent health evidence on the role of fractions, chemical constituents and sources of emission. Inhal. Toxicol. 25 (14), 802–812. https://doi.org/10.3109/08958378.2013.850127. ⟨https://www.ncbi.nlm.nih.gov/pubmed/24304307⟩.

Claxton, L.D., 2015. The history, genotoxicity, and carcinogenicity of carbon-based fuels and their emissions. Part 3: diesel and gasoline. Mutat. Res. Rev. 763, 30–85. https://doi.org/10.1016/j.mrrev.2014.09.002. ⟨https://www.ncbi.nlm.nih.gov/pubmed/25795114⟩.

Dandajeh, H.A., Ladommatos, N., Hellier, P., Eveleigh, A., 2017. Effects of unsaturation of C-2 and C-3 hydrocarbons on the formation of PAHs and on the toxicity of soot particles. Fuel 194, 306–320. https://doi.org/10.1016/j.fuel.2017.01.015. <Go to ISI>://WOS:000394064400032.

Dandajeh, H.A., Ladommatos, N., Hellier, P., Eveleigh, A., 2018. Influence of carbon number of C-1-C-7 hydrocarbons on PAH formation. Fuel 228, 140–151. https://doi.org/10.1016/j.fuel.2018.04.133. <Go to ISI>://WOS:000438190500015.

Delfino, R.J., 2002. Epidemiologic evidence for asthma and exposure to air toxics: linkages between occupational, indoor, and community air pollution research (doi:). Environ. Health Perspect. 110, 573–589. https://doi.org/10.1289/ehp.02110s4573.

Douki, T., Corbiere, C., Preterre, D., Martin, P.J., Lecureur, V., Andre, V., et al., 2018. Comparative study of diesel and biodiesel exhausts on lung oxidative stress and genotoxicity in rats. Environ. Pollut. 235, 514–524. https://doi.org/10.1016/j.envpol.2017.12.077. ⟨https://www.ncbi.nlm.nih.gov/pubmed/29324381⟩.

Efthymiopoulos, I., Hellier, P., Ladommatos, N., Mills-Lamptey, B., 2019. Transesterification of high-acidity spent coffee ground oil and subsequent combustion and emissions characteristics in a compression-ignition engine. Fuel 247, 257–271. https://doi.org/10.1016/j.fuel.2019.03.040. <Go to ISI>://WOS:000463823800027.

Epa U. Development of a relative potency factor (RPF) approach for polycyclic aromatic hydrocarbon (PAH) mixtures. External review draft. 2010;EPA/635/R-08/012A.

Eveleigh, A., Ladommatos, N., Hellier, P., Jourdan, A.L., 2015. An investigation into the conversion of specific carbon atoms in oleic acid and methyl oleate to particulate matter in a diesel engine and tube reactor. Fuel 153, 604–611. https://doi.org/10.1016/j.fuel.2015.03.037. <Go to ISI>://WOS:000352800800069.

Eveleigh, A., Ladommatos, N., Hallier, P., Jourdan, A.L., 2016. Quantification of the fraction of particulate matter derived from a range of C-13-labeled fuels blended into heptane, studied in a diesel engine and tube reactor. Energy Fuel 30 (9), 7678–7690. https://doi.org/10.1021/acs.energyfuels.6b00322. <Go to ISI>://WOS:000383641000087.

Fransen, L.F.H., Leonard, M.O., 2021. CD34+ derived macrophage and dendritic cells display differential responses to paraquat. Toxicol. Vitr. 75, 105198 https://doi.org/10.1016/j.tiv.2021.105198. ⟨https://www.ncbi.nlm.nih.gov/pubmed/34097952⟩.
Fukagawa, N.K., Li, M., Poynter, M.E., Palmer, B.C., Parker, E., Kasumba, J., et al., 2013. Soy biodiesel and petrodiesel emissions differ in size, chemical composition and stimulation of inflammatory responses in cells and animals. Environ. Sci. Technol. 47 (21), 12496–12504. https://doi.org/10.1021/es403146c. ⟨https://www.ncbi.nlm.nih.gov/pubmed/24053625⟩.
Fulcher, M.L., Randell, S.H., 2013. Human nasal and tracheo-bronchial respiratory epithelial cell culture. Methods Mol. Biol. 945, 109–121. https://doi.org/10.1007/978-1-62703-125-7_8. ⟨https://www.ncbi.nlm.nih.gov/pubmed/23097104⟩.
Hellier, P., Ladommatos, N., 2015. The influence of biodiesel composition on compression ignition combustion and emissions. P I Mech. Eng. -J. Pow. 229 (7), 714–726. https://doi.org/10.1177/0957650915598424. <Go to ISI>://WOS:000364167700003.
Hellier, P., Talibi, M., Eveleigh, A., Ladommatos, N., 2018. An overview of the effects of fuel molecular structure on the combustion and emissions characteristics of compression ignition engines. P I Mech. Eng. D. -J. Aut. 232 (1), 90–105. https://doi.org/10.1177/0954407016687453. <Go to ISI>://WOS:000425991000007.
Hellier, P., Jamil, F., Zaglis-Tyraskis, E., Al-Muhtaseb, A.H., Al Haj, L., Ladommatos, N., 2019. Combustion and emissions characteristics of date pit methyl ester in a single cylinder direct injection diesel engine. Fuel 243, 162–171. https://doi.org/10.1016/j.fuel.2019.01.022. <Go to ISI>://WOS:000459431800018.
Hill, W., Lim, E.L., Weeden, C.E., Lee, C., Augustine, M., Chen, K., et al., 2023. Lung adenocarcinoma promotion by air pollutants. Nature 616 (7955), 159–167. https://doi.org/10.1038/s41586-023-05874-3. ⟨https://www.ncbi.nlm.nih.gov/pubmed/37020004⟩.
Houten, S.M., Auwerx, J., 2004. PGC-1alpha: turbocharging mitochondria. Cell 119 (1), 5–7. https://doi.org/10.1016/j.cell.2004.09.016. ⟨https://www.ncbi.nlm.nih.gov/pubmed/15454076⟩.
Jayaratne, E.R., He, C., Ristovski, Z.D., Morawska, L., Johnson, G.R., 2008. A comparative investigation of ultrafine particle number and mass emissions from a fleet of on-road diesel and CNG buses. Environ. Sci. Technol. 42 (17), 6736–6742. https://doi.org/10.1021/es800394x. <Go to ISI>://WOS:000258883300069.
Karavalakis, G., Bakeas, E., Stournas, S., 2010. Influence of oxidized biodiesel blends on regulated and unregulated emissions from a diesel passenger car. Environ. Sci. Technol. 44 (13), 5306–5312. https://doi.org/10.1021/es100831j. <Go to ISI>://WOS:000279304700076.
Karavalakis, G., Gysel, N., Schmitz, D.A., Cho, A.K., Sioutas, C., Schauer, J.J., et al., 2017. Impact of biodiesel on regulated and unregulated emissions, and redox and proinflammatory properties of PM emitted from heavy-duty vehicles. Sci. Total Environ. 584, 1230–1238. https://doi.org/10.1016/j.scitotenv.2017.01.187. <Go to ISI>://WOS:000399358500121.
Khan, Z.A., Hellier, P., Ladommatos, N., 2022. Measurement of soot mass and PAHs during the pyrolysis of C-2-C-4 alcohols at high temperatures. Combust. Flame 236 doi: ARTN 11180310.1016/j.combustflame.2021.111803. <Go to ISI>://WOS:000717213600004.
Kuenen J., Dellaert, S., Visschedijk, A., Jalkanen, J.-P., Super, I. and Denier van der Gon, H. Copernicus Atmosphere Monitoring Service regional emissions version 5.1 business-as-usual CAMS-REG-v51 BAU 2020 (doi:1024380/eptm-kn40). 2021; doi: 10.24380/eptm-kn40.
Lag, M., Ovrevik, J., Refsnes, M., Holme, J.A., 2020. Potential role of polycyclic aromatic hydrocarbons in air pollution-induced non-malignant respiratory diseases. Respir. Res. 21 (1), 299. https://doi.org/10.1186/s12931-020-01563-1. ⟨https://www.ncbi.nlm.nih.gov/pubmed/33187512⟩.
Lapuerta, M., Armas, O., Rodriguez-Fernandez, J., 2008. Effect of biodiesel fuels on diesel engine emissions. Prog. Energy Combust. 34 (2), 198–223. https://doi.org/10.1016/j.pecs.2007.07.001. <Go to ISI>://WOS:000254147400003.
Lee, W.S., Ham, W., Kim, J., 2021. Roles of NAD(P)H:quinone oxidoreductase 1 in diverse diseases. Life 11 (12). https://doi.org/10.3390/life11121301. ⟨https://www.ncbi.nlm.nih.gov/pubmed/34947831⟩.
Li, N., Georas, S., Alexis, N., Fritz, P., Xia, T., Williams, M.A., et al., 2016. A work group report on ultrafine particles (American Academy of Allergy, Asthma & Immunology): why ambient ultrafine and engineered nanoparticles should receive special attention for possible adverse health outcomes in human subjects. J. Allergy Clin. Immun. 138 (2), 386–396. https://doi.org/10.1016/j.jaci.2016.02.023. <Go to ISI>://WOS:000380835800007.
Li, Z., Jiang, W., Chu, H., Ge, J., Wang, X., Jiang, J., et al., 2022. Exploration of potential mechanism of interleukin-33 up-regulation caused by 1,4-naphthoquinone black carbon in RAW264.7 cells. Sci. Total Environ. 835, 155357 https://doi.org/10.1016/j.scitotenv.2022.155357. ⟨https://www.ncbi.nlm.nih.gov/pubmed/35452731⟩.
Liu, D., 1981. A rapid biochemical test for measuring chemical toxicity. Bull. Environ. Contam. Toxicol. 26 (2), 145–149. https://doi.org/10.1007/BF01622068. ⟨https://www.ncbi.nlm.nih.gov/pubmed/7248535⟩.
Llamas, A., Al-Lal, A.M., Garcia-Martinez, M.J., Ortega, M.F., Llamas, J.F., Lapuerta, M., et al., 2017. Polycyclic aromatic hydrocarbons (PAHs) produced in the combustion of fatty acid alkyl esters from different feedstocks: quantification, statistical analysis and mechanisms of formation. Sci. Total Environ. 586, 446–456. https://doi.org/10.1016/j.scitotenv.2017.01.180. <Go to ISI>://WOS:000398758800043.
Madden, M.C., 2016. A paler shade of green? The toxicology of biodiesel emissions: recent findings from studies with this alternative fuel. BBA-Gen. Subj. 1860 (12), 2856–2862. https://doi.org/10.1016/j.bbagen.2016.05.035. <Go to ISI>://WOS:000384866700010.
Mehus, A.A., Reed, R.J., Lee, V.S., Littau, S.R., Hu, C., Lutz, E.A., et al., 2015. Comparison of acute health effects from exposures to diesel and biodiesel fuel emissions. J. Occup. Environ. Med. 57 (7), 705–712. https://doi.org/10.1097/JOM.0000000000000473. ⟨https://www.ncbi.nlm.nih.gov/pubmed/26147538⟩.
Meldrum, K., Gant, T.W., Macchiarulo, S., Leonard, M.O., 2016. Bronchial epithelial innate and adaptive immunity signals are induced by polycyclic aromatic hydrocarbons. Toxicol. Res. 5 (3), 816–827. https://doi.org/10.1039/c5tx00389j. ⟨https://www.ncbi.nlm.nih.gov/pubmed/30090392⟩.
Meldrum, K., Gant, T.W., Leonard, M.O., 2017. Diesel exhaust particulate associated chemicals attenuate expression of CXCL10 in human primary bronchial epithelial cells. Toxicol. Vitr. 45 (3), 409–416. https://doi.org/10.1016/j.tiv.2017.06.023. ⟨https://www.ncbi.nlm.nih.gov/pubmed/28655636⟩.
Meldrum, K., Robertson, S., Romer, I., Marczylo, T., Gant, T.W., Smith, R., et al., 2020. Diesel exhaust particle and dust mite induced airway inflammation is modified by cerium dioxide nanoparticles. Environ. Toxicol. Pharm. 73, 103273 https://doi.org/10.1016/j.etap.2019.103273. ⟨https://www.ncbi.nlm.nih.gov/pubmed/31629203⟩.
Moorthy, B., Chu, C., Carlin, D.J., 2015. Polycyclic aromatic hydrocarbons: from metabolism to lung cancer. Toxicol. Sci. 145 (1), 5–15. https://doi.org/10.1093/toxsci/kfv040. ⟨https://www.ncbi.nlm.nih.gov/pubmed/25911656⟩.
Ning, X., Ji, X., Li, G., Sang, N., 2019. Ambient PM2.5 causes lung injuries and coupled energy metabolic disorder. Ecotoxicol. Environ. Saf. 170, 620–626. https://doi.org/10.1016/j.ecoenv.2018.12.028. ⟨https://www.ncbi.nlm.nih.gov/pubmed/30579162⟩.
Nisbet, I.C., LaGoy, P.K., 1992. Toxic equivalency factors (TEFs) for polycyclic aromatic hydrocarbons (PAHs). Regul. Toxicol. Pharmacol. 16 (3), 290–300. https://doi.org/10.1016/0273-2300(92)90009-x. ⟨https://www.ncbi.nlm.nih.gov/pubmed/1293646⟩.
Ogbunuzor, C.C., Hellier, P.R., Talibi, M., Ladommatos, N., 2021. In-cylinder polycyclic aromatic hydrocarbons sampled during diesel engine combustion. Environ. Sci. Technol. 55 (1), 571–580. https://doi.org/10.1021/acs.est.0c05561. ⟨https://www.ncbi.nlm.nih.gov/pubmed/33295764⟩.
Ostby, L., Engen, S., Melbye, A., Eide, I., 1997. Mutagenicity testing of organic extracts of diesel exhaust particles after fractionation and recombination. Arch. Toxicol. 71 (5), 314–319. https://doi.org/10.1007/s002040050392. ⟨https://www.ncbi.nlm.nih.gov/pubmed/9137810⟩.
Pardo, M., Qiu, X., Zimmermann, R., Rudich, Y., 2020. Particulate matter toxicity is Nrf2 and mitochondria dependent: the roles of metals and polycyclic aromatic hydrocarbons. Chem. Res. Toxicol. 33 (5), 1110–1120. https://doi.org/10.1021/acs.chemrestox.0c00007. ⟨https://www.ncbi.nlm.nih.gov/pubmed/32302097⟩.
Parliament E. Directive 2009/28/EC - Renewable Energy Directive. European Parliament and Council. 2009;L 140:16–62.
Peirce, D.M., Alozie, N.S.I., Hatherill, D.W., Ganippa, L.C., 2013. Premixed burn fraction: its relation to the variation in NOx emissions between petro- and biodiesel. Energy Fuel 27 (7), 3838–3852. https://doi.org/10.1021/ef4006719. <Go to ISI>://WOS:000322150200027.
Post, S., Nawijn, M.C., Hackett, T.L., Baranowska, M., Gras, R., van Oosterhout, A.J., et al., 2012. The composition of house dust mite is critical for mucosal barrier dysfunction and allergic sensitisation. Thorax 67 (6), 488–495. https://doi.org/10.1136/thoraxjnl-2011-200606. ⟨https://www.ncbi.nlm.nih.gov/pubmed/22167364⟩.
Propper, R., Wong, P., Bui, S., Austin, J., Vance, W., Alvarado, A., et al., 2015. Ambient and emission trends of toxic air contaminants in California. Environ. Sci. Technol. 49 (19), 11329–11339. https://doi.org/10.1021/acs.est.5b02766. ⟨https://www.ncbi.nlm.nih.gov/pubmed/26340590⟩.
Reynolds, A.S., Pierre, T.H., McCall, R., Wu, J., Gato, W.E., 2018. Evaluating the cytotoxicity of tin dioxide nanofibers. J. Environ. Sci. Health A Toxic Hazard Subst. Environ. Eng. 53 (11), 986–991. https://doi.org/10.1080/10934529.2018.1471024. ⟨https://www.ncbi.nlm.nih.gov/pubmed/29775400⟩.
Ryu, M.H., Lau, K.S., Wooding, D.J., Fan, S., Sin, D.D., Carlsten, C., 2020. Particle depletion of diesel exhaust restores allergen-induced lung-protective surfactant protein D in human lungs. Thorax 75 (8), 640–647. https://doi.org/10.1136/thoraxjnl-2020-214561. ⟨https://www.ncbi.nlm.nih.gov/pubmed/32467339⟩.
Samburova, V., Zielinska, B., Khlystov, A., 2017. Do 16 polycyclic aromatic hydrocarbons represent PAH air toxicity? Toxics 5 (3). https://doi.org/10.3390/toxics5030017. ⟨https://www.ncbi.nlm.nih.gov/pubmed/29051449⟩.
Schonborn, A., Ladommatos, N., Williams, J., Allan, R., Rogerson, J., 2009. The influence of molecular structure of fatty acid monoalkyl esters on diesel combustion. Combust. Flame 156 (7), 1396–1412. https://doi.org/10.1016/j.combustflame.2009.03.011. <Go to ISI>://WOS:000266857300010.
Shahir, V.K., Jawahar, C.P., Suresh, P.R., 2015. Comparative study of diesel and biodiesel on CI engine with emphasis to emissions-A review. Renew. Sustain Energy Rev. 45, 686–697. https://doi.org/10.1016/j.rser.2015.02.042. <Go to ISI>://WOS:000351963400052.
Shvedova, A.A., Yanamala, N., Murray, A.R., Kisin, E.R., Khaliullin, T., Hatfield, M.K., et al., 2013. Oxidative stress, inflammatory biomarkers, and toxicity in mouse lung and liver after inhalation exposure to 100% biodiesel or petroleum diesel emissions. J. Toxicol. Environ. Health A 76 (15), 907–921. https://doi.org/10.1080/15287394.2013.825217. ⟨https://www.ncbi.nlm.nih.gov/pubmed/24156694⟩.
Silverman, D.T., 2018. Diesel exhaust and lung cancer-aftermath of becoming an IARC group 1 carcinogen. Am. J. Epidemiol. 187 (6), 1149–1152. https://doi.org/10.1093/aje/kwy036. ⟨https://www.ncbi.nlm.nih.gov/pubmed/29522191⟩.
Smargiassi, A., Goldberg, M.S., Wheeler, A.J., Plante, C., Valois, M.F., Mallach, G., et al., 2014. Associations between personal exposure to air pollutants and lung function tests and cardiovascular indices among children with asthma living near an industrial complex and petroleum refineries. Environ. Res. 132, 38–45. https://doi.org/10.1016/j.envres.2014.03.030. <Go to ISI>://WOS:000337862300007.
Southern, D., Hellier, P., Talibi, M., Leonard, M.O., Ladommatos, N., 2021. Re-assessing the toxicity of particles from biodiesel combustion: a quantitative analysis of in vitro

studies. Atmos. Environ. 261 doi: ARTN 11857010.1016/j.atmosenv.2021.118570. <Go to ISI>://WOS:000687041300001.

Stevens, E.L., Rosser, F., Han, Y.Y., Forno, E., Acosta-Perez, E., Canino, G., et al., 2020. Traffic-related air pollution, dust mite allergen, and childhood asthma in Puerto Ricans. Am. J. Respir. Crit. Care Med. 202 (1), 144–146. https://doi.org/10.1164/rccm.201912-2325LE. ⟨https://www.ncbi.nlm.nih.gov/pubmed/32197046⟩.

Su, J.Y., Zhu, H.Y., Bohac, S.V., 2013. Particulate matter emission comparison from conventional and premixed low temperature combustion with diesel, biodiesel and biodiesel-ethanol fuels. Fuel 113, 221–227. https://doi.org/10.1016/j.fuel.2013.05.068. <Go to ISI>://WOS:000323937300026.

Talibi, M., Hellier, P., Ladommatos, N., 2018. Impact of increasing methyl branches in aromatic hydrocarbons on diesel engine combustion and emissions. Fuel 216, 579–588. https://doi.org/10.1016/j.fuel.2017.12.045. <Go to ISI>://WOS:000427818100062.

Tree, D.R., Svensson, K.I., 2007. Soot processes in compression ignition engines. Prog. Energy Combust. 33 (3), 272–309. https://doi.org/10.1016/j.pecs.2006.03.002. <Go to ISI>://WOS:000246327800002.

Tsai, J.H., Huang, K.L., Chiu, C.H., Lin, C.C., Kuo, W.C., Lin, W.Y., et al., 2011. Particle-bound PAHs and particle-extract-induced cytotoxicity of emission from a diesel-generator fuelled with soy-biodiesel. Aerosol Air Qual. Res. 11 (7), 822–836. https://doi.org/10.4209/aaqr.2011.08.0119. <Go to ISI>://WOS:000298004300004.

Unosson, J., 2014. Acute Cardiovascular Effects of Biofuel Exhaust Exposure. Umeå University. ⟨https://www.diva-portal.org/smash/record.jsf?pid=diva2%3A764764&dswid=-5569⟩.

Unosson, J., Kabele, M., Boman, C., Nystrom, R., Sadiktsis, I., Westerholm, R., et al., 2021. Acute cardiovascular effects of controlled exposure to dilute Petrodiesel and biodiesel exhaust in healthy volunteers: a crossover study. Part Fibre Toxicol. 18 (1), 22. https://doi.org/10.1186/s12989-021-00412-3. ⟨https://www.ncbi.nlm.nih.gov/pubmed/34127003⟩.

Winship, K.A., 1988. Toxicity of tin and its compounds. Advers. Drug React. Acute Poison Rev. 7 (1), 19–38. ⟨https://www.ncbi.nlm.nih.gov/pubmed/3291572⟩.

Wu, J.T., Song, K.H., Litzinger, T., Lee, S.Y., Santoro, R., Linevsky, M., et al., 2006. Reduction of PAH and soot in premixed ethylene-air flames by addition of ethanol. Combust. Flame 144 (4), 675–687. https://doi.org/10.1016/j.combustflame.2005.08.036. <Go to ISI>://WOS:000236192100003.

Xia, T., Korge, P., Weiss, J.N., Li, N., Venkatesen, M.I., Sioutas, C., et al., 2004. Quinones and aromatic chemical compounds in particulate matter induce mitochondrial dysfunction: implications for ultrafine particle toxicity. Environ. Health Perspect. 112 (14), 1347–1358. https://doi.org/10.1289/ehp.7167. ⟨https://www.ncbi.nlm.nih.gov/pubmed/15471724⟩.